Pathways for practical high-energy long-cycling lithium metal batteries

Jun Liu [1]*, Zhenan Bao [2], Yi Cui [2], Eric J. Dufek [3], John B. Goodenough [4], Peter Khalifah [5], Qiuyan Li [1], Bor Yann Liaw [3], Ping Liu [6], Arumugam Manthiram [4], Y. Shirley Meng [6], Venkat R. Subramanian [1,7], Michael F. Toney [8], Vilayanur V. Viswanathan [1], M. Stanley Whittingham [9], Jie Xiao [1], Wu Xu [1], Jihui Yang [7], Xiao-Qing Yang [5] and Ji-Guang Zhang [1]

State-of-the-art lithium (Li)-ion batteries are approaching their specific energy limits yet are challenged by the ever-increasing demand of today's energy storage and power applications, especially for electric vehicles. Li metal is considered an ultimate anode material for future high-energy rechargeable batteries when combined with existing or emerging high-capacity cathode materials. However, much current research focuses on the battery materials level, and there have been very few accounts of cell design principles. Here we discuss crucial conditions needed to achieve a specific energy higher than 350 Wh kg^{-1}, up to 500 Wh kg^{-1}, for rechargeable Li metal batteries using high-nickel-content lithium nickel manganese cobalt oxides as cathode materials. We also provide an analysis of key factors such as cathode loading, electrolyte amount and Li foil thickness that impact the cell-level cycle life. Furthermore, we identify several important strategies to reduce electrolyte-Li reaction, protect Li surfaces and stabilize anode architectures for long-cycling high-specific-energy cells.

Lithium (Li)-ion batteries have had a profound impact on modern society[1]. Over the past 25 years, the specific energy of Li-ion batteries has steadily increased while their cost has dramatically decreased. However, the electric vehicle energy-storage market demands an even higher specific energy, to more than 500 Wh kg^{-1} at the cell level, and a lower cost, below US\$100 (kWh)$^{-1}$ at the pack level[2]. At present, many approaches are being pursued in developing next-generation high-energy batteries, such as Li-oxygen and Li-sulfur batteries[2–4]. All solid-state batteries also have received widespread attention due to their inherent high safety characteristics[5]. Among these approaches, Li metal is considered a key component to achieving a higher specific energy than that of today's Li-ion technology. Most studies so far have focused on characterization and mitigation of dendrite formation on the material level[6–8]. Although there have been some studies on new cell architectures with improved performances[9] and on properties of pouch cells[10], there have been very few reports on how the many new materials and concepts studied in the literature should be incorporated into a practical high-energy cell with specific energy higher than 300 Wh kg^{-1} and what is needed to improve the cell-level energy density and cycle life of practical rechargeable Li metal batteries.

Here we provide a cell-level analysis of what we consider to be the crucial conditions for a rechargeable Li metal battery to achieve a specific energy higher than 350 Wh kg^{-1}, up to 500 Wh kg^{-1}, using a high-capacity cathode such as a high-nickel-content lithium nickel manganese cobalt oxide (high-Ni NMC) (Ni ≥ 60%) based on a pouch-cell format. We discuss the cell-level parameters required to increase the cell energy and cycle life. Rather than providing a complete review or summary of the properties of and advances on

the Li metal anode, cathode or electrolyte, we highlight the factors that cause the cell to fail in short cycle life and limit the efficient utilization of the full capacity of the active materials, and identify key strategies to extend the cycle life of the full cells.

Material requirements for 500 Wh kg^{-1} practical cells

To develop the most feasible approach to build the highest-specific-energy cells, we consider the best cathode and anode candidates that are available in large quantities for cell fabrication at an industrial scale. Among the known anode materials, Li metal has an ultrahigh theoretical specific capacity (3,860 mAh g^{-1}) and an extremely low standard electrochemical redox potential (−3.040 V versus the standard hydrogen electrode), and therefore is considered one of the most important anode materials for future energy storage systems[11]. Among the reported lithium intercalation cathode materials[1], we select high-Ni NMC (LiNi$_x$M$_{1-x}$O$_2$, M = Mn, Co and $x \geq 0.6$) based on the consideration of its capacity (greater than 200 mAh g^{-1}), operating voltage (ca. 3.8 V) and commercial availability. Other emerging cathode materials can be explored in the future for even higher specific capacities, including sulfur or oxygen[3,4], metal fluoride materials[12], lithium-rich manganese-rich layered oxide materials[13] and anion redox cathode materials[14].

A commercially viable cell needs to meet many requirements, including high specific energy, long cycle life, good mechanical and chemical stability over a wide range of temperature, safe operation, and so on. As a starting point, this Perspective analyses the crucial conditions of the cell parameters required for a high-energy cell using a Li||high-Ni NMC (>1 Ah) pouch-cell format containing multiple layers of current collectors, anodes, separators and

[1]Energy and Environment Directorate, Pacific Northwest National Laboratory, Richland, WA, USA. [2]Department of Materials Science and Engineering, Stanford University, Stanford, CA, USA. [3]Clean Energy and Transportation Division, Idaho National Laboratory, Idaho Falls, ID, USA. [4]Department of Mechanical Engineering, The University of Texas at Austin, Austin, TX, USA. [5]Chemistry Division, Brookhaven National Laboratory, Upton, NY, USA. [6]Department of NanoEngineering, University of California, San Diego, CA, USA. [7]College of Engineering, University of Washington, Seattle, WA, USA. [8]Stanford Synchrotron Radiation Lightsource, SLAC National Accelerator Laboratory, Menlo Park, CA, USA. [9]Department of Materials Science and Engineering, Binghamton University, Binghamton, NY, USA. *e-mail: jun.liu@pnnl.gov
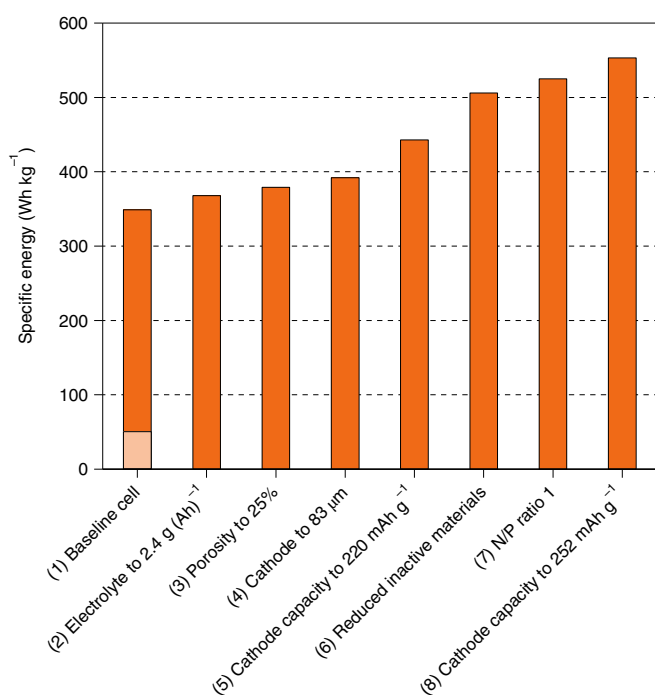
Fig. 1 | Calculated cell-level specific energy as a function of cell parameters. (1) A baseline NMC622 material with 196 mAh g^{-1} specific capacity (charge cut-off at 4.6 V), 35% cathode porosity, 22.0 mg cm^{-2} cathode mass loading and 70 µm cathode thickness. The N/P ratio is 2.6 and the electrolyte to capacity ratio is 3.0 g (Ah)$^{-1}$. The lightly shaded area in the baseline cell represents a specific energy much less than 50 Wh kg^{-1} based on the amount of the cathode, anode and electrolyte and other inactive materials reported in most literature studies for rechargeable coin cells. (2) Reducing the amount of electrolyte (electrolyte to capacity ratio) to 2.4 g (Ah)$^{-1}$. (3) Reducing the cathode porosity to 25% so further reducing the electrolyte amount to 2.1 g (Ah)$^{-1}$. (4) Increasing the cathode thickness to 83 µm and mass loading to 26.0 mg cm^{-2} thus increasing the specific capacity of the whole cathode. (5) Increasing the cathode capacity to 220 mAh g^{-1}. (6) Reducing inactive materials (current collector, packaging) by more than 50%. (7) Reducing the Li to N/P ratio of 1. (8) Using hypothetical new cathode materials with a capacity much higher than 250 mAh g^{-1}. See the Methods for the selections of cell parameters and the calculations of specific energies.

cathodes. The pouch cell is chosen because it is one of the most common cell formats in commercial production with high manufacturing flexibility.

To integrate the best material properties with the optimal cell design parameters to achieve a specific energy up to 500 Wh kg^{-1}, we plotted the cell-level specific energy under different scenarios to illustrate the feasible pathways to different targets (Fig. 1). The cell-level specific energy is calculated by multiplying the total cathode capacity and the cell voltage (taken as the mid-point voltage in discharge), and then dividing by the total mass of the pouch cell. For the baseline cell, parameters similar to a typical Li-ion battery are used. These baseline parameters, including the cathode thickness, porosity, amount of electrolytes and so on, represent what can be reasonably implemented in the pouch-cell fabrication based on knowledge from Li-ion cells and thus serve as a starting point for our analysis. The challenge is to optimize these parameters to reach the desired specific energy while still achieving good cycle life in practical Li metal cells. Figure 1 shows the upper limit of the specific energy when those key parameters are pushed to the limit.

The first bar in Fig. 1 shows that a specific energy of about 350 Wh kg^{-1} for a Li||LiNi$_{0.6}$Mn$_{0.2}$Co$_{0.2}$O$_2$ (Li||NMC622) pouch cell can be obtained by using the baseline cell parameters. Key parameters such as the cathode porosity (35%) and thickness (70 µm) are based on what can be easily achieved in the current Li-ion pouch-cell fabrication. The electrolyte amount (represented by the electrolyte to cell-capacity ratio) is higher than what would be used in a typical Li-ion cell using graphite anodes considering the inherent interaction and consumption of the electrolyte with the Li metal anode, but the electrolyte to capacity ratio of 3.0 g (Ah)$^{-1}$ reflects the maximum amount of the electrolyte allowed for the 350 Wh kg^{-1} cell. The cell specific energy can be further increased by reducing the amount of electrolyte (Fig. 1, second bar), reducing the porosity (Fig. 1, third bar) and increasing the cathode thickness (Fig. 1, fourth bar). However, a severe reduction in the electrolyte amount may result in a significant penalty in the cycle life[15,16], unless effective measures are discovered to reduce unwanted side reactions. In addition, state-of-the-art electrode fabrication techniques are expected to limit the cathode loading to about 25% porosity and the thickness to less than 100 µm for the NMC materials. To achieve more than 400 Wh kg^{-1} with the current cell design, the cathode materials need to have a stable specific capacity of about 220 mAh g^{-1} (Fig. 1, fifth bar), which remains an ongoing research target for the community. Additional improvement in specific energy can be made by significant reduction of the inactive material content (Cu, Al, separator and packaging) (Fig. 1, sixth bar), and by significant reduction of Li amount (Fig. 1, seventh bar). The effect of inactive materials will not be a main focus of discussion. The Li amount, shown as the negative/positive electrode areal capacity ratio (N/P ratio) in the analysis, is limited by the availability of reliable Li foils (about 50 µm thick) today. Further reduction the N/P ratio is obviously desired. Finally, if new cathode materials with a specific capacity more than 250 mAh g^{-1} can be developed in the future, a cell-level specific energy over 500 Wh kg^{-1} can be obtained (Fig. 1, eighth bar). The Methods provides further details on the selection of cell parameters and the calculations of specific energies.

Factors affecting cycle life in high-energy cells
Long cycle life of Li metal electrodes has been reported by many groups on the coin-cell level with a large excess amount of Li metal and flooded electrolyte[10,15]. However, most of these results cannot be translated to a practical pouch cell, which requires the use of minimal Li metal and electrolyte. The parameters reported in most studies for rechargeable coin cells will produce a specific energy much less than 50 Wh kg^{-1} based on the amount of the cathode, anode and electrolyte and other inactive materials required (lightly shaded area in the baseline cell in Fig. 1). As illustrated in Fig. 2, key cell parameters, including cathode loading, electrolyte amount and Li metal amount (thickness), have serious effects on the cycling performance. It is imperative to carefully choose these parameters, in addition to other inactive materials, such as separators, current collectors and packaging materials, to achieve a long-cycling high-energy practical cell.

For practical cells with a specific energy of more than 300 Wh kg^{-1}, the amount of electrolyte used in this Perspective is 3 g (Ah)$^{-1}$. However, in most previous reports about Li metal batteries with long lifetimes in CR2032 coin cells, the electrolyte amount was in a flooded state (75 µl or more)[4]. Assuming that the cathode loading in these coin cells is 1 mAh cm^{-2} on a 1.3 cm^2 electrode, the 75 µl electrolyte translates to an electrolyte/capacity ratio of ~70 g (Ah)$^{-1}$, 23 times higher than the electrolyte content typically used in a pouch cell. Figure 2c shows that reducing the electrolyte amount from 25 to 3 g (Ah)$^{-1}$ drastically reduced the cycle life to ~10 cycles.

In addition to electrolyte amount, the Li abundance also plays a key role. With a thick Li foil, the dominant failure mechanism is electrolyte consumption from solid electrolyte interphase (SEI)
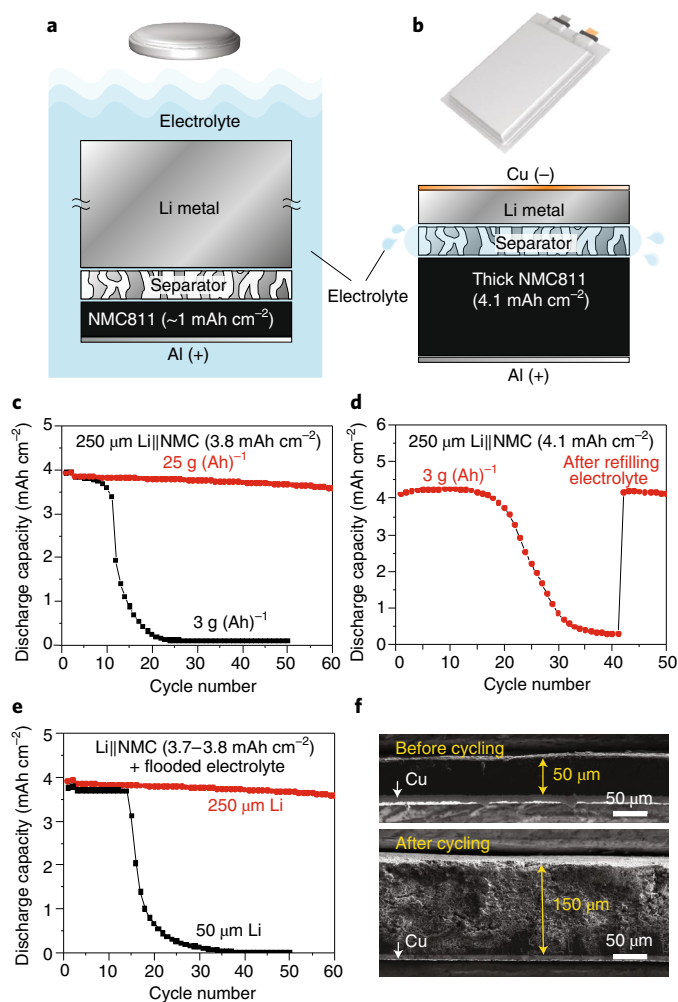
Fig. 2 | Relation between cell parameters and cell cycle life and Li anode morphologies. a, Lab coin cells often use unlimited amounts of Li and electrolytes and cannot reflect the conditions in operating practical Li metal cells. **b,** High-energy pouch cells with multiple stacked layers of electrodes; here only one unit is displayed for comparison with the coin cell configuration. **c–e,** Cycling performance of Li||NMC cells with different electrolyte amounts (**c**), with electrolyte replenished after the original lean electrolyte was consumed (**d**) and with different amounts (that is, thicknesses) of Li metal (**e**). **f,** Thickness change of Li metal anode after cycling for the cell in **e** with 50-μm-thick Li. Note that the cells for **c–f** were tested in coin-type cells with controlled parameters at the Pacific Northwest National Laboratory. The coin cells for **c–e** were conducted for two formation cycles at C/10 rate followed by cycling at C/3 rate for both charge and discharge processes in the voltage range of 2.7–4.4 V.

formation reactions. Under such conditions, the cell capacity can be recovered by replenishing the electrolyte (Fig. 2d). The Li anodes typically used in laboratory testing are very thick (250 μm or more) and are thus five times the thickness of the Li anode (50 μm) required to reach a high energy of 300 Wh kg^{-1}. Figure 2e shows that even with abundant electrolytes, the cycle life may be reduced to less than 20 cycles when the Li foil thickness is limited to 50 μm. These results clearly suggest that the rapid degradation mechanism in early stages is due to the electrolyte and Li consumption, not dendrite formation. This is substantiated by a scanning electron microscope image of the Li foil after long cycling, which shows the formation of very thick, porous and mossy Li structures throughout the electrode thickness (Fig. 2f). The thickness of 50 μm Li tripled after only tens of cycles indicating that the whole Li anode

probably participates in the electrochemical and chemical reactions. Furthermore, the cathode loading is also very important. The low cathode loading (1 mAh cm^{-2} or less) utilized in most previous studies leads to very 'shallow' stripping/deposition of Li in the same cell, which artificially leads to long cycle life that will not translate to high-energy-density cell designs.

Strategies for long-cycling high-energy cells

Fundamentally, the effects of the key parameters controlling cell lifetime are all related to Li-electrolyte interfacial reactions[15]. In a practical cell with high cathode loading, lean electrolyte and thin Li, the fast failure is directly derived from the production of thick porous SEI structures on the Li metal (Fig. 2f), whose formation causes both electrolyte and Li metal depletion. This process leads to pulverization of Li metal and cell swelling, which not only limits the cycle life of the anode but also raises safety concerns. Two processes are involved in the formation of the detrimental Li microstructure. The first is the formation of a heterogeneous SEI layer, which is a self-amplifying process initiated by the inherent instability of the electrolyte at very reductive potentials and the inhomogeneous surface chemistry and accelerated by uneven distribution of the resulting electric field (Fig. 3a)[6]. The second process is Li dendrite formation (Fig. 3b–d)[17]. The steep concentration gradients at the Li/electrolyte interface accelerate the growth of long, fibrous, dendritic Li[18], which has a high risk of shorting the cells. Therefore any strategy to extend the cycle life of the high-energy Li metal cell should include fundamental studies to understand the complex interplay between SEI and Li metal, which leads to decomposition and depletion of electrolytes, production of thick porous SEI structures and 'inactive' Li that no longer participates in the electrochemical reactions, and large volumetric expansion of the anode (Fig. 3c,d). At present, there is no single and simple solution for these Li metal problems in a high-energy cell. We now discuss four key strategies to address the challenges of Li metal in high-energy cells.

Quantitative analysis on cycled Li metal anodes. Although Li dendrite formation has been studied for a long time, the complex Li loss processes under aggressive electrochemical conditions in practical cells have received less attention. Coulombic efficiency is widely reported and used to quantify the Li reaction[19,20]. However, the cycle life measured in a cell can be much shorter or sometimes longer than predicted by Coulombic efficiency, depending on the specific conditions of the measurements[21].

The key to understanding the cycle life is the differentiation and quantification of various forms of Li (including the Li$^+$ ions in the SEI layer and the electrochemically inactive metallic Li trapped by the SEI), and their distribution and evolution on the continuous cycling. Unfortunately, it is challenging to apply most analytical techniques to study Li metal because of its high chemical reactivity and low stability[7]. This is particularly pronounced for in situ investigations. Recently, cryogenic transmission electron microscopy was used ex situ to reveal the atomic structure, the nanoscale composition and the growth mechanism of electrochemically deposited Li metal[7,8]. Cryo-transmission electron microscopy can be used for direct observation of dendrite formation and the structure of electrochemically deposited Li metal[8], the atomic structures of SEI layers[7] and the fate of various kinds of Li metal anodes[22]. However, obtaining real-time, quantitative information remains quite challenging.

The combination of electrochemical, chemical measurements and advanced characterization techniques will be the most effective way to obtain information on the electrochemical reactions, but such investigations should be conducted in situ under experimental conditions mimicking the cell parameters discussed earlier. For example, in most reports, the Coulombic efficiency was measured using Li metal and Cu counter electrodes[20]. To use the Coulombic
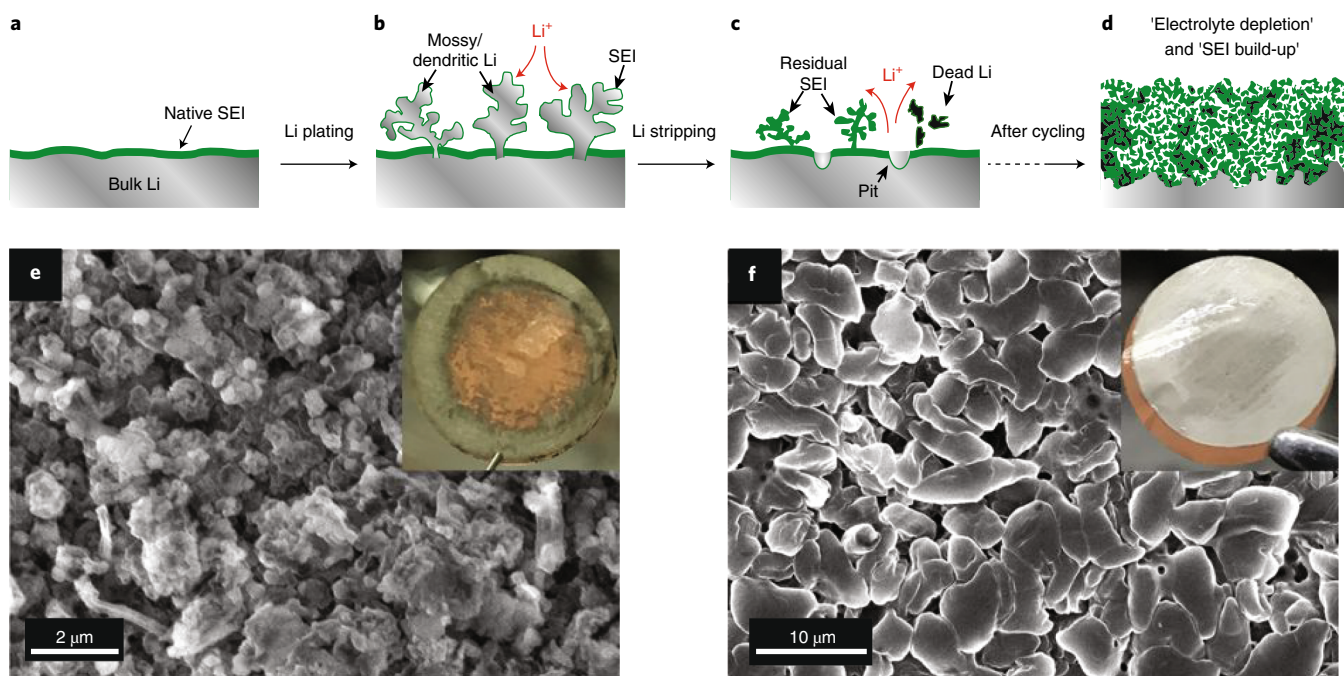
Fig. 3 | Illustration of major failure mechanisms in Li metal anodes. a, Pristine Li metal anode with uneven surface and initial SEI. **b**, Mossy/dendritic Li formation during Li deposition. **c**, Formation of residual SEI, 'dead' Li and pits on Li anode during Li stripping. **d**, Interplay between Li and SEI that depletes the electrolyte and corrodes the Li metal anode. **e**, Highly porous fine Li films with carbonate electrolytes. **f**, Denser, coarse Li film deposited with improved electrolytes. Panels **e** and **f** reproduced from ref. [49], Springer Nature Ltd.

efficiency obtained in these measurements to predict the cycle life, these measurements should be conducted with high Li metal utilization in a thin Li electrode and a variety of current densities similar to those used in practical pouch cells. In addition, similar measurements should be conducted with limited electrolytes and appropriate cathode materials to understand the effects of high voltage, and cross-over of the decomposition species generated from the cathode[23]. A stable cathode material should be first studied, likely using stable lithium iron phosphate or lithium nickel manganese oxide spinel to decouple the reactions from the cathode materials. Then the measurements should be conducted with high-Ni NMC or other cathode materials useful for practical applications. Furthermore, advanced techniques such as in situ X-ray nanoprobe and microdiffraction (Fig. 4a), should be developed to provide qualitative and quantitative information on how much electrolyte is consumed, how much Li metal is reacted and in what form, the nature of the Li reaction products that are no longer electrochemically active (inactive Li), and the chemical and physical characteristics of the SEI layers on the Li surface.

Furthermore, experimental work should be bolstered with advanced modelling concepts that take into account the suite of different conditions, which include chemical, mechanical and electrochemical aspects. The development of such models will need to include macroscale, moving boundaries, microstructure evolution, detailed kinetics, fundamental quantification of plasticity and nucleation to arrive at a multiscale model to quantify the effect of operating conditions on the performance of Li anodes.

New electrolytes and additives. To date, the most effective strategy exploited to mitigate the SEI formation and extend the cell-level cycle life has been the development of new electrolytes to improve Li deposition/stripping. The cell cycle life can be greatly extended by this approach[24]. Different electrolytes lead to different morphologies of deposited Li, from dendritic to fibrous, columnar or granular (Fig. 4b)[25]. A deposition process that produces dense Li is essential

to reduce surface area and suppress the SEI reactions[7,26]. Additives such as $CsPF_6$ (ref. [27]) or even a trace amount of H_2O (ref. [28]) or $LiAsF_6$ (ref. [29]) have demonstrated the ability to tune the SEI qualities, and have led to more uniform deposition of Li morphology in the early stage of cycling. However, it is possible that once the additive is consumed, the entangled Li and SEI reactions will resume and deplete both electrolyte and Li metal. Other electrolyte additives that promote the formation of alloy phases have also been demonstrated, but the effectiveness of such approaches remains to be studied under high-Li-consumption conditions[30].

One promising approach is to use the super-concentrated Li salts in electrolytes[31]. The high salt concentration could accelerate mass transport in the electrolyte, reduce the concentration gradient formed at the Li/electrolyte interface and mitigate dendrite growth[31]. In addition, the large number of Li cations coordinates with the solvent molecules, which reduces the electrolyte reactivity against the Li metal. However, it is difficult to directly use a highly concentrated electrolyte for building a practical cell because it increases the viscosity, reduces the charge transport kinetics, and increases the cost and the difficulty of cell fabrication. Recent reports have demonstrated that a co-solvent that does not solvate Li^{+} but has good miscibility with the solvating solvent could function as a 'diluent' in highly concentrated electrolytes. The 'diluent' addition can well maintain the properties of the high salt concentration and greatly reduce the salt concentration, the viscosity and the cost of the final electrolyte[24,32]. This concept of 'localized high concentration electrolyte' has recently been further expanded to non-flammable inorganic phosphate-based electrolytes[33]. The Li metal deposited in highly concentrated electrolytes and localized high concentration electrolytes has a much smoother surface and larger nodule sizes, compared with the porous Li structure produced using conventional electrolytes (Fig. 3e,f at a low current density). However, the electrolytes studied so far could not completely prevent the formation of a porous Li layer. A more systematic approach should be developed to explore a wide range of salts and additives to improve the stability
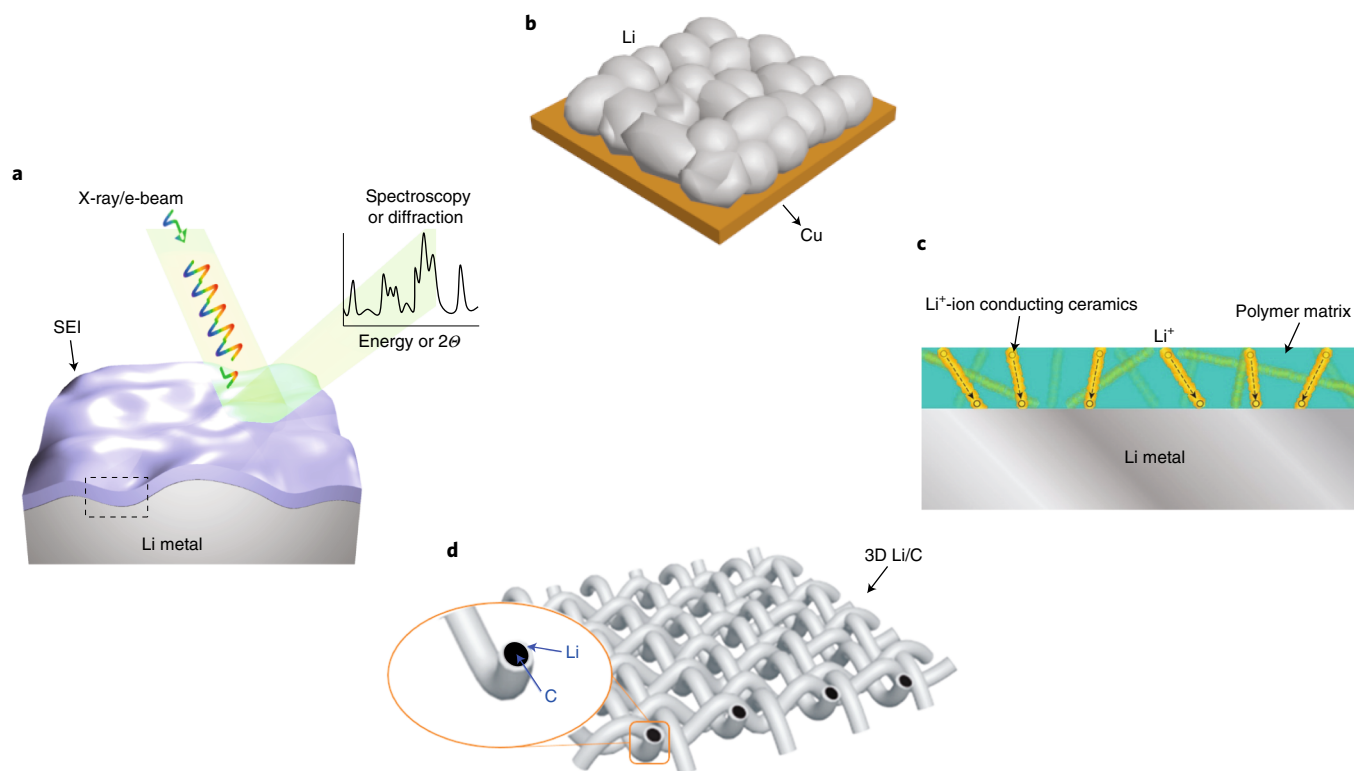
Fig. 4 | Solutions proposed in the literature to characterize and mitigate Li metal problems. a, Schematic of in situ X-ray nanoprobe/micro-diffraction to differentiate the consumption of Li through interfacial reaction or the formation of dead Li. **b**, Desired morphology of deposited Li in dense and granular shapes that can be regulated by newly developed electrolytes and additives. **c**, Adaptive protective layer of polymeric/ceramic composite electrolyte to prevent contact of Li metal and liquid electrolyte and to suppress Li dendrites. **d**, Three-dimensional (3D) host architecture to stabilize Li anodes.

of the electrolytes towards Li metal, and promote dense Li deposition. High-throughput experimental/computational tools[34] could be used to more rapidly identify effective additives, salts and conditions for stable and dense Li deposition.

Li metal protection. Solid electrolytes can protect the Li metal from interacting with electrolytes and pave the way for significantly reduced electrolyte volumes or future 'solid-state batteries'. Solid-state electrolytes, including solid polymers[35], ceramic electrolytes[36] and polymer/ceramic composites[37,38], are being intensively studied. Based on the Monroe–Newman model, it is expected that a solid-state electrolyte with a high shear modulus — at least twice that of Li metal — can effectively suppress Li dendrites[39]. Although many groups are focusing on ceramic membranes, alternative cell formats and manufacturing processes have been investigated[9,38]. The key to preventing 'short circuits' with a ceramic electrolyte such as garnet densified at a high temperature is to have a uniform interface[40]. Rather than using rigid solid electrolyte protection, polymer, block copolymer or composite electrolytes have been widely studied[41,42]. The polymer materials are not only flexible for easy manufacturing, but also provide additional functionalities such as self-healing[43]. One of the most widely studied polymers is polyethylene oxide (PEO) and its derivatives due to the flexibility of these polymer chains[44]. Still, it is hard to achieve sufficient ionic conductivity in PEO-based polymers below 60 °C unless they are solvated by the electrolyte, under which conditions the electrolyte and Li metal reactions still occur to a large extent.

Overall, a high-energy cell requires a very thin (less than 10 μm), flexible and strong solid electrolyte with good Li ion conductivity and good stability and compatibility with the liquid electrolyte, the cathode and anode materials. Most solid electrolyte materials studied in the literature are not quite ready to be implemented in a high-energy cell due to various reasons. One significant factor is that many materials are only prepared and studied as very thick films (sometimes over 100 μm). The state-of-the-art separators are less than 10 μm already. Using thick films, whether ceramics or polymers, will dramatically diminish the cell-level energy density. A very thin homogeneous film, whether formed in situ or ex situ, is desired (Fig. 4c). Mechanically and electrochemically stable polymers, such as fluorinated or aromatic polymers, should be considered. The ionic conductivity of these polymers should not be dependent on the solvation of the electrolyte. Therefore new ion transport mechanisms need to be explored that do not completely rely on polymer segment relaxation[44]. An elegant approach was reported recently that relies on the ionic conductivity of the single particles embedded in a polymer film[45]. The single particle approach is interesting because it could eliminate the effect of the grain boundaries on the ion transport properties. This study points to the direction of using low-dimensional materials such as single crystalline nanowires in a composite film. Intensive investigation is needed to identify the appropriate conducting phase and the desired architecture (particle or domain size, morphology, orientation and distribution) for optimum mechanical and electrochemical properties. The role of the interfaces in the composite materials in promoting or inhibiting the Li ion conductivity and dendrite formation should be carefully investigated.

Thin Li anode and architectures. As discussed, one of the key reasons for the unstable cycling of Li cells is the large volumetric change of the anode structure. There are two approaches to mitigate this effect. One is to use very thin Li. This thickness needs to be reduced to less than 20 μm. The second approach is to develop a stable and

conductive Li host that can be used to minimize the volume changes or 'swelling/shrinking' of Li during cycling, and effectively reduce the local current density (Fig. 4d). Similar to the Li ion insertion into a graphite or a hard carbon material, the Li metal can be deposited on and stripped from the stable host structure without causing much dimensional change. Three-dimensional-structured Li metal anodes by using hosts of carbon (C), porous Cu and porous polymer membranes have been investigated to increase the anode stability and cycle life of the Li metal electrode[9,46,47]. In particular, Li/C composite architectures have attracted wide attention[48]. However, there have been no reports of successful use of such host structures under realistic conditions required for practical high-energy cells. A host structure naturally introduces voids and additional weight of the inactive materials. Therefore the thickness, the porosity and the relative amount of host material with respect to the Li should be minimized for practical uses. To achieve a cell-level specific energy higher than 350 Wh kg^{-1}, the mass ratio of Li to C host should be larger than 1, while keeping high cathode loading, lean electrolyte and small N/P ratio that need to be used as discussed above. In addition to these requirements, most methods used to prepare the C hosts are not scalable for large-area production for cell fabrication and testing. Dedicated efforts are needed for infiltration, coating, stacking, tabbing and sealing of an anode structure containing very thin porous hosts during cell fabrication.

Outlook

Developing a long-cycling, high-energy rechargeable Li metal battery pushes almost all the parameters to their limits. Effective methods must be developed to enable the use and long-cycling of a Li anode in a practical cell with high cathode loading, lean electrolyte and limited N/P ratio. Understanding the cell-level failure mechanisms can be facilitated by new measurement techniques and characterization tools to fully quantify the reactions of the active and inactive Li during cycling. Better electrolytes and electrolyte additives using concepts of concentrated electrolytes or localized high concentration electrolytes are effective in reducing the reactivity towards the electrolyte, but significant research is still needed to promote a dense, not porous Li deposition. Ultrathin, flexible solid electrolytes are desirable to separate the Li metal from the electrolyte. Mechanical and electrochemically stable polymers other than PEO should be studied. A future high-energy Li metal battery will also most likely use a very thin Li layer, and possible Li host structure as the anode, but the Li host structures must be within the boundaries of the cell design parameters, and the host structures must be scalable and compatible for cell manufacturing.

Ultimately, the development of a commercially viable rechargeable Li metal battery adequate for electric vehicles and other consumer applications depends on not only achieving high specific energy and long cycle life, but also demonstrating safety and reliability. We hope that this Perspective will draw attention to the fact that more efforts are needed on cell-level problems so that new developments and advances can be more aligned with the requirements of the performance of the cells and new materials can be more rapidly implemented.

Methods

Calculation of cell-level specific energies. This method part gives detailed explanations of the specific energies shown in Fig. 1 in the main text, which depicts the variation of the specific energy of a cell as a function of different cell parameters with a fixed negative/positive electrode areal capacity ratio (N/P ratio) and gives the upper limit of the achievable specific energy of Li||high-Ni NMC pouch cells. The specific energy (E_{Sp}, in Wh kg^{-1}) of a cell can be calculated as

$$E_{Sp} = C_{Cell} \times V_{Cell} / W_{Cell} \qquad (1)$$

where C_{Cell} is the cell capacity (in Ah), V_{Cell} is the cell voltage (in V) and W_{Cell} is the total cell weight (in kg). C_{Cell} is correlated to the specific capacity of the cathode material and the loading of the cathode when the anode is in excess in capacity,

that is, C_{Cell} (Ah) = C_{SpCath} (Ah kg^{-1}) × W_{Cath} (kg). V_{Cell} is normally defined as the mid-point voltage during the discharge process. W_{Cell} includes the weights of all components used to build the whole cell such as the active materials (cathode material, Li anode and electrolyte) and the inactive materials (conductive carbon, binder, current collectors, tabs, separator and packaging material). To achieve a practical Li metal battery, all cell parameters similar to those used in traditional Li-ion cells have been used. In this work, cell dimensions were based on the pouch-cell configuration used at the Pacific Northwest National Laboratory, that is, length 70.0 mm, width 41.5 mm and thickness up to 4.5 mm.

As a starting point, the LiNi$_{0.6}$Mn$_{0.2}$Co$_{0.2}$O$_2$ (NMC622) cathode was chosen to build the Li metal pouch cell. When the Li||NMC622 cell was charged to 4.6 V, the specific capacity of NMC622 of 196 mAh g^{-1} and an average mid-point discharge voltage of 3.89 V could be obtained. The NMC622 cathode was made of active material of 96%, conductive carbon 2% and binder 2%, and had an areal mass loading of about 22 mg cm^{-2} for a single side on an Al foil of 12 μm thickness. The cathode was calendared to a single side thickness of 70 μm to yield a density of 3.1 g cm^{-3} and a porosity of 35%. In the Li||NMC622 cell, the ratio of the areal capacity of negative electrode (Li) to the areal capacity of positive electrode (NMC622), that is, N/P ratio, was set at 2.4. A Cu foil of 6 μm thickness was used for the Li metal anode. The pouch cell was assembled at a 20 layer construction. Considering the electrolyte to capacity ratio in commercial Li-ion batteries is roughly 1.3–1.5 g (Ah)$^{-1}$, and the facts of the high reactivity of Li metal and the electrolyte as well as of the porous Li formed after deposition and redeposition, an electrolyte to capacity ratio of 3.0 g (Ah)$^{-1}$ was used. By controlling the weights of current collectors and packaging material, a baseline specific energy of about 350 Wh kg^{-1} at the cell level could be obtained from the calculation of 2.26 Ah × 3.89 V / 0.0252 kg, which is the specific energy used in the first bar in Fig. 1.

When the same ratios of electrodes, electrolyte and current collectors were used in CR2032 coin cells, but just the packaging material (including the spacer and the spring) was changed to stainless steel, the specific energy of the coin cell was less than 50 Wh kg^{-1}, which is shown as the lightly shaded area in the first bar in Fig. 1.

For the second bar in Fig. 1, the cell parameters used in the pouch cell of the first bar in Fig. 1 were kept the same except for the reduction in electrolyte amount. The electrolyte to capacity ratio of 2.4 g (Ah)$^{-1}$ was chosen for this calculation. Of course, another electrolyte to capacity ratio, such as 2.6 g (Ah)$^{-1}$ or 2.3 g (Ah)$^{-1}$, could be used but it should not be lower than the 1.3–1.5 g (Ah)$^{-1}$ value, which is used in conventional Li-ion batteries. It is seen that the specific energy can be increased to 368 Wh kg^{-1} (= 2.26 Ah × 3.89 V / 0.0239 kg) by reducing the electrolyte amount due to the decrease of the total cell weight.

Similarly, based on the cell parameters in the second bar of Fig. 1 but by reducing the cathode porosity from 35% to less than 25% (normally the porosity less than 20% is very difficult to achieve), the utilization of electrolyte amount can be further reduced. Here, we chose an electrolyte to capacity ratio of 2.1 g (Ah)$^{-1}$ for the case of porosity reduction to 25%. Certainly, the specific energy of the Li||NMC622 pouch cell can be further increased to 379 Wh kg^{-1} (= 2.26 Ah × 3.89 V / 0.0232 kg) (Fig. 1, third bar).

For the fourth bar in Fig. 1, based on the cell parameters used of the third bar in Fig. 1 and by increasing the cathode loading (cathode thickness to more than 80 μm, on each side of the current collector) one can actually increase the active material amount in the cathode so as to increase the cell capacity. In this case, the mass loading of the active material in the cathode was increased from 22.0 to 26.0 mg cm^{-2}. Then the specific energy of the Li||NMC622 pouch cell was increased to ca. 392 Wh kg^{-1} (= 2.66 Ah × 3.89 V / 0.0264 kg).

If a higher-Ni-content NMC cathode, for example, LiNi$_{0.8}$Mn$_{0.1}$Co$_{0.1}$O$_2$ (NMC811) with a specific capacity of ca. 220 mAh g^{-1} was used, thus reducing the N/P ratio to 2, together with the above mentioned other parameters, it is possible to design a cell with a specific energy of more than 400 Wh kg^{-1}. For the fifth bar of Fig. 1, the specific energy of 442 Wh kg^{-1} was obtained from the calculation of 2.98 Ah × 3.89 V / 0.0262 kg.

The cell design for more than 500 Wh kg^{-1} cell requires more than 50% reduction of the amount of Li metal and the inactive materials (Cu, Al and packaging). When reducing the weight of inactive materials (such as conductive carbon, binder, Al and Cu current collectors, separator and packaging material) used in the Li||NMC811 cell in the fifth bar of Fig. 1, the cathode areal loading was slightly increased so the cell capacity was slightly increased; at the same time, the cell polarization was reduced, thus the average discharge voltage was slightly increased too. Then the specific energy of the cell could be further improved to ca. 506 Wh kg^{-1} (= 3.19 Ah × 3.93 V / 0.0248 kg) (Fig. 1, sixth bar). Furthermore, when reducing the N/P ratio to 1 and maintaining the other parameters used for the sixth bar in Fig. 1 cell, the specific capacity of the cell could be increased to 525 Wh kg^{-1} (= 3.19 Ah × 3.93 V / 0.0239 kg) (Fig. 1, seventh bar).

Of course, if new cathode materials with a more than 250 mAh g^{-1} specific capacity can be developed in the future, without sacrificing the voltage, packing density, stability and other parameters we discussed in this Perspective, more than 500 Wh kg^{-1} specific energy can be obtained. In the eighth bar of Fig. 1, the specific capacity of the cell could be increased to 552 Wh kg^{-1} (= 3.64 Ah × 3.93 V / 0.0259 kg).

References

1. Whittingham, M. S. Ultimate limits to intercalation reactions for lithium batteries. *Chem. Rev.* **114**, 11414–11443 (2014).
2. Van Noorden, R. A better battery. *Nature* **507**, 26–28 (2014).
3. Xia, C., Kwok, C. Y. & Nazar, L. F. A high-energy-density lithium-oxygen battery based on a reversible four-electron conversion to lithium oxide. *Science* **361**, 777–781 (2018).
4. Fang, R. et al. More reliable lithium-sulfur batteries: status, solutions and prospects. *Adv. Mater.* **29**, 1606823 (2017).
5. Wu, B. et al. Interfacial behaviours between lithium ion conductors and electrode materials in various battery systems. *J. Mater. Chem. A* **4**, 15266–15280 (2016).
6. Wu, B., Lochala, J., Taverne, T. & Xiao, J. The interplay between solid electrolyte interface (SEI) and dendritic lithium growth. *Nano Energy* **40**, 34–41 (2017).
7. Wang, X. et al. New insights on the structure of electrochemically deposited lithium metal and its solid electrolyte interphases via cryogenic TEM. *Nano Lett.* **17**, 7606–7612 (2017).
8. Li, Y. et al. Atomic structure of sensitive battery materials and interfaces revealed by cryo-electron microscopy. *Science* **358**, 506–510 (2017).
9. Yang, C. et al. Continuous plating/stripping behavior of solid-state lithium metal anode in a 3D ion-conductive framework. *Proc. Natl Acad. Sci. USA* **115**, 3770–3775 (2018).
10. Kim, M. S. et al. Langmuir–Blodgett artificial solid-electrolyte interphases for practical lithium metal batteries. *Nat. Energy* **3**, 889–898 (2018).
11. Xu, W. et al. Lithium metal anodes for rechargeable batteries. *Energy Environ. Sci.* **7**, 513–537 (2014).
12. Pohl, A. et al. Development of a water based process for stable conversion cathodes on the basis of FeF$_3$. *J. Power Sources* **313**, 213–222 (2016).
13. Li, X. et al. Fundamental insight into Zr modification of Li- and Mn-rich cathodes: combined transmission electron microscopy and electrochemical impedance spectroscopy study. *Chem. Mater.* **30**, 2566–2573 (2018).
14. Zhu, Z. et al. Anion-redox nanolithia cathodes for Li-ion batteries. *Nat. Energy* **1**, 16111 (2016).
15. Yu, L. et al. A localized high-concentration electrolyte with optimized solvents and lithium difluoro(oxalato)borate additive for stable lithium metal batteries. *ACS Energy Lett.* **3**, 2059–2067 (2018).
16. Nagpure, S. C. et al. Impacts of lean electrolyte on cycle life for rechargeable Li metal batteries. *J. Power Sources* **407**, 53–62 (2018).
17. Elezgaray, J., Léger, C. & Argoul, F. Linear stability analysis of unsteady galvanostatic electrodeposition in the two-dimensional diffusion-limited regime. *J. Electrochem. Soc.* **145**, 2016–2024 (1998).
18. Bai, P., Li, J., Brushett, F. R. & Bazant, M. Z. Transition of lithium growth mechanisms in liquid electrolytes. *Energy Environ. Sci.* **9**, 3221–3229 (2016).
19. Burns, J. C. et al. Predicting and extending the lifetime of Li-ion batteries. *J. Electrochem. Soc.* **160**, A1451–A1456 (2013).
20. Adams, B. D., Zheng, J., Ren, X., Xu, W. & Zhang, J. G. Accurate determination of Coulombic efficiency for lithium metal anodes and lithium metal batteries. *Adv. Energy Mater.* **8**, 1702097 (2018).
21. Suo, L. et al. Fluorine-donating electrolytes enable highly reversible 5-V-class Li metal batteries. *Proc. Natl Acad. Sci. USA* **115**, 1156–1161 (2018).
22. Zachman, M. J., Tu, Z., Choudhury, S., Archer, L. A. & Kourkoutis, L. F. Cryo-STEM mapping of solid–liquid interfaces and dendrites in lithium-metal batteries. *Nature* **560**, 345–349 (2018).
23. Li, J., Li, W., You, Y. & Manthiram, A. Extending the service life of high-Ni layered oxides by tuning the electrode–electrolyte interphase. *Adv. Energy Mater.* **8**, 1801957 (2018).
24. Chen, S. et al. High-voltage lithium-metal batteries enabled by localized high-concentration electrolytes. *Adv. Mater.* **30**, 1706102 (2018).
25. Liu, B., Zhang, J.-G. & Xu, W. Advancing lithium metal batteries. *Joule* **2**, 833–845 (2018).
26. Zheng, J. et al. Electrolyte additive enabled fast charging and stable cycling lithium metal batteries. *Nat. Energy* **2**, 17012 (2017).
27. Ding, F. et al. Dendrite-free lithium deposition via self-healing electrostatic shield mechanism. *J. Am. Chem. Soc.* **135**, 4450–4456 (2013).
28. Qian, J. et al. Dendrite-free Li deposition using trace-amounts of water as an electrolyte additive. *Nano Energy* **15**, 135–144 (2015).
29. Ren, X. et al. Guided lithium metal deposition and improved lithium Coulombic efficiency through synergistic effects of LiAsF$_6$ and cyclic carbonate additives. *ACS Energy Lett.* **3**, 14–19 (2018).
30. Liang, X. et al. A facile surface chemistry route to a stabilized lithium metal anode. *Nat. Energy* **2**, 17119 (2017).
31. Qian, J. et al. High rate and stable cycling of lithium metal anode. *Nat. Commun.* **6**, 6362 (2015).
32. Ren, X. et al. Localized high-concentration sulfone electrolytes for high-efficiency lithium-metal batteries. *Chem* **4**, 1877–1892 (2018).
33. Chen, S. et al. High-efficiency lithium metal batteries with fire-retardant electrolytes. *Joule* **2**, 1548–1558 (2018).
34. Cheng, L. et al. Accelerating electrolyte discovery for energy storage with high-throughput screening. *J. Phys. Chem. Lett.* **6**, 283–291 (2015).
35. Khurana, R., Schaefer, J. L., Archer, L. A. & Coates, G. W. Suppression of lithium dendrite growth using cross-linked polyethylene/poly(ethylene oxide) electrolytes: a new approach for practical lithium-metal polymer batteries. *J. Am. Chem. Soc.* **136**, 7395–7402 (2014).
36. Choudhury, S., Mangal, R., Agrawal, A. & Archer, L. A. A highly reversible room-temperature lithium metal battery based on crosslinked hairy nanoparticles. *Nat. Commun.* **6**, 10101 (2015).
37. Orsini, F. et al. In situ scanning electron microscopy (SEM) observation of interfaces within plastic lithium batteries. *J. Power Sources* **76**, 19–29 (1998).
38. Han, X. et al. Negating interfacial impedance in garnet-based solid-state Li metal batteries. *Nat. Mater.* **16**, 572–579 (2017).
39. Monroe, C. & Newman, J. The impact of elastic deformation on deposition kinetics at lithium/polymer interfaces. *J. Electrochem. Soc.* **152**, A396–A404 (2005).
40. Cheng, E. J., Sharafi, A. & Sakamoto, J. Intergranular Li metal propagation through polycrystalline Li$_{6.25}$Al$_{0.25}$La$_3$Zr$_2$O$_{12}$ ceramic electrolyte. *Electrochim. Acta* **223**, 85–91 (2017).
41. Long, L., Wang, S., Xiao, M. & Meng, Y. Polymer electrolytes for lithium polymer batteries. *J. Mater. Chem. A* **4**, 10038–10069 (2016).
42. Gomez, E. D. et al. Effect of ion distribution on conductivity of block copolymer electrolytes. *Nano Lett.* **9**, 1212–1216 (2009).
43. Liu, K. et al. Lithium metal anodes with an adaptive "solid–liquid" interfacial protective layer. *J. Am. Chem. Soc.* **139**, 4815–4820 (2017).
44. Wang, Y. & Sokolov, A. P. Design of superionic polymer electrolytes. *Curr. Opin. Chem. Eng.* **7**, 113–119 (2015).
45. Aetukuri, N. B. et al. Flexible ion-conducting composite membranes for lithium batteries. *Adv. Energy Mater.* **5**, 1500265 (2015).
46. Ye, H. et al. Stable Li plating/stripping electrochemistry realized by a hybrid Li reservoir in spherical carbon granules with 3D conducting skeletons. *J. Am. Chem. Soc.* **139**, 5916–5922 (2017).
47. Liang, Z. et al. Composite lithium metal anode by melt infusion of lithium into a 3D conducting scaffold with lithiophilic coating. *Proc. Natl Acad. Sci. USA* **113**, 2862–2867 (2016).
48. Zhang, Y. et al. High-capacity, low-tortuosity, and channel-guided lithium metal anode. *Proc. Natl Acad. Sci. USA* **114**, 3584–3589 (2017).
49. Zeng, Z. et al. Non-flammable electrolytes with high salt-to-solvent ratios for Li-ion and Li-metal batteries. *Nat. Energy* **3**, 674–681 (2018).

Competing interests

The authors declare no competing interests.

Additional information

Reprints and permissions information is available at www.nature.com/reprints.

Correspondence should be addressed to J.L.

Publisher's note: Springer Nature remains neutral with regard to jurisdictional claims in published maps and institutional affiliations.